Perspective

From Static to Dynamic: Rethinking Interface Passivation in Inverted Perovskite Solar Cells

Qingyun Xiao [1], Xiaofen Jiang [2], Xiaonan Wang [2,3], Qinggui Li [2,3], Rui Wang [2], and Jingjing Xue [3,*]

[1] Department of Electronic and Information Engineering, School of Engineering, Westlake University, Hangzhou 310024, China
[2] Department of Materials Science and Engineering, School of Engineering, Westlake University, Hangzhou 310024, China
[3] State Key Laboratory of Silicon and Advanced Semiconductor Materials, School of Materials Science and Engineering, Zhejiang University, Hangzhou 310027, China
* Correspondence: jjxue@zju.edu.cn

Received: 30 January 2026; Revised: 3 March 2026; Accepted: 23 March 2026; Published: 25 March 2026

Abstract: Interface passivation is central to efficiency improvement in inverted perovskite solar cells, yet its effectiveness is fundamentally limited by the assumption of a static picture. Herein, we argue that the perovskite/electron transport layer interface is intrinsically dynamic under operation, continuously evolving under illumination, thermal stress, and electrical bias owing to ion migration, interfacial redistribution, passivator destabilization, and chemical reactions. These coupled processes progressively reconstruct interfacial energetics and defect landscapes, leading to voltage loss, fill-factor decay, hysteresis re-emergence, and irreversible performance degradation even in devices with high initial efficiencies. By reframing the interface as a time-dependent system rather than a fixed structure, this perspective highlights dynamic interfacial evolution as the origin of long-term instability and calls for interface regulation strategies that prioritize sustained functional stability under realistic operating conditions.

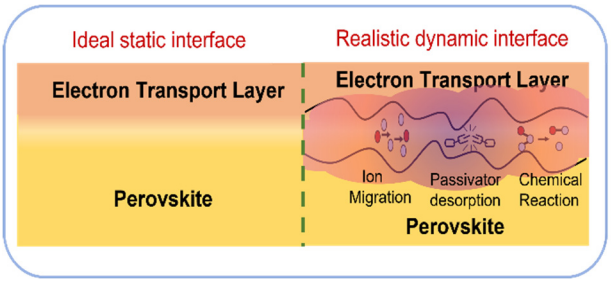

Keywords: dynamic interface; interface passivation; ion migration; operational stability; interfacial evolution

1. Introduction

Over the past decade, organic-inorganic halide perovskite solar cells (PSCs) have demonstrated an unprecedented increase in power conversion efficiency (PCE). This progress has emerged from coordinated advances in materials composition regulation, thin-film fabrication processing, and increasingly refined interface engineering [1]. Among these efforts, passivation of the contact interface between the perovskite absorber and the electron transport layer (ETL) has attracted particular attention [2]. By implementing a variety of interface passivation approaches, non-radiative recombination at the perovskite/ETL interface can be substantially suppressed, leading to measurable improvements in both the open-circuit voltage (V_{OC}) and fill factor (FF) [3]. These passivation approaches have contributed decisively to the rapid efficiency improvements achieved in laboratory-scale devices, underscoring the increasingly prominent role of interface engineering in advancing the performance of PSCs [4].

However, the achievement of high efficiency does not inherently ensure stable performance under prolonged operational conditions, a phenomenon that has been consistently observed across a wide range of device architectures and material systems. Even devices featuring rigorously engineered and well-passivated interfaces often exhibit gradual performance degradation during continuous illumination, thermal stress, or electrical bias [5]. This discrepancy between efficiency and stability indicates that prevailing interface engineering strategies, while highly effective at improving static performance indicators, remain insufficient in sustaining device functionality over extended timescales. Implicitly, the most existing approaches are founded on the assumption that an interface optimized at fabrication remains structurally and electronically static throughout device operation.

Such a static interface assumption, however, is fundamentally incompatible with the intrinsic physical characteristics of halide perovskites. Owing to their soft lattices and pronounced ion mobility, the distribution of ions, defect configurations, and local electrostatic modulations at perovskite surfaces and near-interface regions are inherently susceptible to gradual reorganization under external stimuli, including illumination, electric fields, and thermal stress [6]. In contrast, ETLs are predominantly composed of organic semiconductors with constrained ion migration and comparatively rigid structures, whose electronic structure and chemical composition change much more slowly during device operation [7]. This asymmetry in structural flexibility and kinetic responsiveness between the two contacting materials renders the perovskite/ETL interface a natural locus for the redistribution of charge carriers, mobile ions, and localized electric potentials.

Under sustained operating conditions, the combined effects of photoexcitation, electrical bias, and thermal stress progressively reshape the interfacial electronic landscape, driving the interface to progressively deviate from the initial configuration. As the interfacial state evolves over time, passivation strategies designed to address a specific, static interface condition may no longer remain chemically or electronically effective. Consequently, interfacial defects can re-emerge or transform, undermining charge extraction and accelerating performance degradation during long-term operation.

This perspective highlights a conceptual gap in prevailing interface engineering: the long-term performance of perovskite solar cells is constrained not merely by incomplete passivation, but by a predominantly static view of an interface that is intrinsically dynamic in nature. Bridging this gap requires a fundamental shift in how to understand and engineer the perovskite/ETL interface, moving beyond its treatment as a static structural entity towards recognizing it as a time-dependent, operating-state-coupled system.

Within this framework, interface passivation should not be regarded solely as a one-time structural modification, but rather as an adaptive process capable of accommodating interfacial evolution under realistic operating conditions. Incorporating this dynamic perspective may provide critical insights into the origins of operational instability, help alleviate existing stability bottlenecks, and ultimately guide perovskite photovoltaics toward practical and commercially viable deployment.

2. Current Interface Passivation Strategy: Achievements and Limitations

Before considering how interface strategies might evolve to accommodate time-dependent interfacial processes, it is instructive to examine the conceptual foundations, achievements, and underlying assumptions of the classical passivation approaches that have dominated the field to date. Such an analysis not only highlights the origins of the remarkable efficiency gains achieved thus far, but also reveals the structural limitations that emerge when these strategies are confronted with realistic operational stress.

Non-radiative recombination and charge-transport losses originating from the perovskite/ETL interface have long been recognized as critical limitations to device performance [8]. As the mechanistic understanding of this interface has deepened, passivation strategies have progressively evolved from isolated defect-repair efforts towards more systematic regulation of interfacial chemical states, electrostatic environments, and structural configurations. Among these, chemical defect passivation represents the most direct and widely adopted approach.

2.1. Chemical Defect Passivation: Local Bonding Optimization

Chemical defect passivation primarily targets the intrinsic atomic-scale imperfections of perovskite surfaces. Extensive theoretical calculations and experimental characterizations consistently indicate that incomplete lattice termination and compositional volatility at perovskite surfaces lead to the accumulation of halide vacancies, under-coordinated Pb^{2+} species, and their associated shallow and deep electronic states, which act as high-density non-radiative recombination centers when located at the perovskite/ETL interface [9]. The introduction of molecules possessing Lewis acid, Lewis base or hydrogen-bonding functionalities enables coordination or electrostatic interactions with these under-coordinated species, effectively saturating dangling bonds and compensating local charge imbalance (Figure 1a). At its core, this strategy seeks to establish a chemically well-terminated perovskite surface at the final stage of device fabrication, characterized by reduced defect density and more idealized stoichiometry and bonding configurations.

2.2. Field-Effect Passivation: Electrostatic Regulation without Direct Defect Elimination

Building upon this understanding, it has become increasingly clear that interfacial recombination losses are not solely governed by point defects that can be eliminated through specific chemical bonding. Long-range electrostatic effects arising from subtle energy-level mismatches, interfacial dipole disorder and inhomogeneous charge distributions can also exert a decisive influence on carrier-transport dynamics in the interfacial region [10].

This recognition has motivated the development of field-effect passivation strategies, which aim to regulate the interfacial electrostatic environment rather than directly modifying atomic-scale defect structures.

By inserting interlayers with tailored electronic structures between the perovskite and the ETL, a predefined local electrostatic potential profile can be established. Whether achieved through interfacial band bending, dipole-induced vacuum-level shifts, or electric double-layer formation, the unifying objective is to reshape carrier-transport pathways such that photogenerated electrons are steered away from recombination-prone regions and efficiently extracted towards the collecting electrode (Figure 1b). Within this framework, defects are not necessarily removed but rendered less active as recombination centers through physical modulation of the carrier-transport environment.

2.3. Structurally Engineered Interfacial Layers: Transitional Architectures

More recently, interface engineering has further progressed from defect- and field-centric strategies toward the deliberate construction of structurally defined interfacial regions. By introducing low-dimensional perovskite layers, molecular cation reconstruction layers, or composite interfacial architectures between the perovskite absorber and the ETL, researchers seek to construct a structurally defined transition region that alleviates abrupt discontinuities in crystal structure, dielectric response, and polarization behavior [11,12].

These engineered interlayers often exhibit ionic distributions and dielectric properties distinct from those of bulk perovskites, enabling partial screening of Coulomb interactions, redistribution of local electric fields, and suppression of interfacial ionic disorder [13]. Through the synergistic integration of defect passivation, energy-level alignment, and electrostatic field remodeling (Figure 1c), such approaches have delivered notable improvements in device efficiency and short-term operational stability.

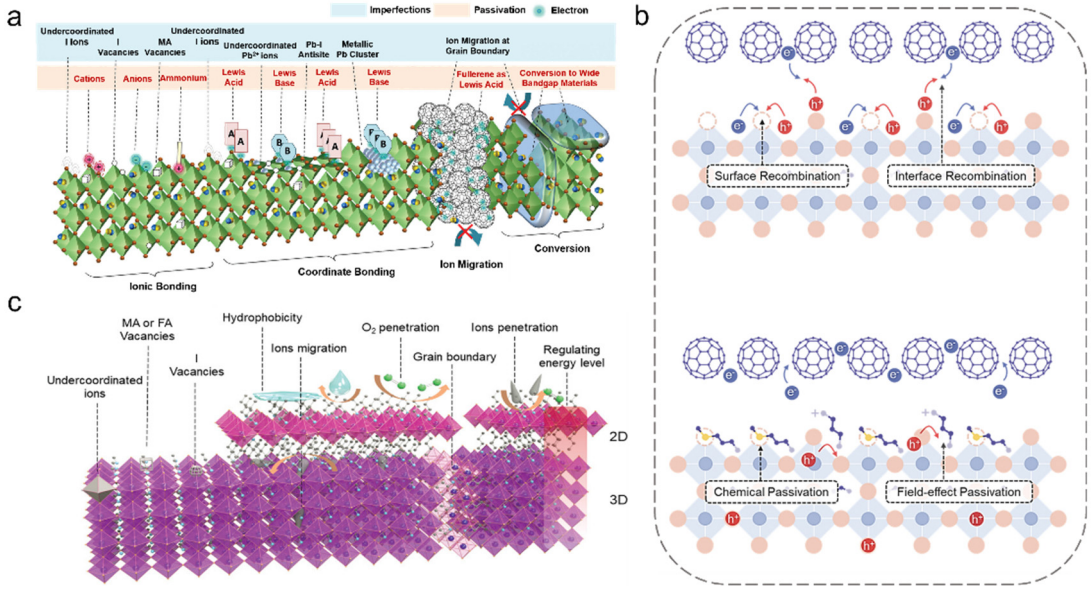

Figure 1. Schematic Diagram of the Current Interface Passivation Strategy Mechanism. (**a**) Imperfections in organic-inorganic halide perovskite film and their passivation by ionic bonding, coordinate bonding, and conversion to wide bandgap materials, and suppression of ion migration at extended defects. Reprinted with permission from Ref. [14]. (**b**) Schematic of the perovskite surface without passivation (**up**) and with diammonium-methylthio dual passivation (DMDP) composed by chemical and field-effect passivation (**down**). Reprinted with permission from Ref. [15]. (**c**) Schematic illustration of the surface passivation using 2D perovskites, in which vacancy/excess defects are well repaired, and the formation of a 2D capping layer with outstanding robustness effectively blocks the penetration of oxygen/moisture. Moreover, the modified energy level facilitates charge transfer and collection. Reprinted with permission from Ref. [16].

2.4. A Shared Paradigm: Static Optimization of a Dynamic Interface

Despite their diverse material implementations and microscopic mechanisms, these classical interface passivation strategies share a common conceptual foundation. They are predominantly implemented during device fabrication or post-treatment stages, with the central objective of maximizing photovoltaic performance by establishing an interfacial configuration that minimizes initial defect density, optimizes energy-level alignment, and suppresses non-radiative

recombination. Consequently, performance assessments typically emphasize post-fabrication gains in V_{OC}, FF and PCE, alongside stability tests conducted under relatively mild and controlled conditions.

Implicit in this framework is the assumption that interface passivation constitutes a largely "one-off" structural optimization, namely that an optimally configured interface established at the outset can be preserved throughout subsequent device operation. This paradigm has been instrumental in enabling the rapid efficiency advances achieved over the past decade and has underpinned sustained progress in interface engineering [17,18].

However, an increasing number of experimental evidence suggests that its implicit premise does not universally hold under realistic operating conditions [19]. Even in devices employing multiple passivation strategies and exhibiting high initial efficiencies, pronounced performance degradation is frequently observed under prolonged illumination, thermal stress, applied electric fields, or their combined influence. Typical manifestations include gradual V_{OC} loss, J_{SC} decay, etc.

3. The Origin and Concrete Manifestations of Dynamic Evolution

From a dynamic viewpoint, the perovskite/ETL interface cannot be regarded as a static entity fixed at the fabrication stage, but rather as an evolving system that continuously responds to external operating environments. Metal halide perovskites possess a soft and adaptive lattice, low activation barriers for ion migration, and metastable surface coordination, making their interfacial structure highly sensitive to temperature, mechanical stress, illumination, and moisture. These external stimuli drive persistent reorganization of lattice geometry, defect populations, and ionic distributions at the interface, progressively shifting it away from its initial equilibrium configuration.

Thermal stimuli induce pronounced lattice expansion, phase transitions, and strain accumulation within the perovskite layer (Figure 2a). Temperature cycling not only alters octahedral tilting and crystal symmetry, but also accelerates ion diffusion and defect activation near the perovskite/ETL interface, leading to dynamically evolving band alignment and interfacial recombination pathways [20].

Similarly, mechanical and lattice mismatch-induced strain further modulates the interfacial energy landscape (Figure 2b). Local strain fields alter Pb-X bond lengths and angles, thereby shifting band edges and lowering the formation energy of defects. This strain-defect coupling creates spatially heterogeneous electronic properties at the interface, enhancing non-radiative recombination and amplifying degradation under prolonged operation [21,22].

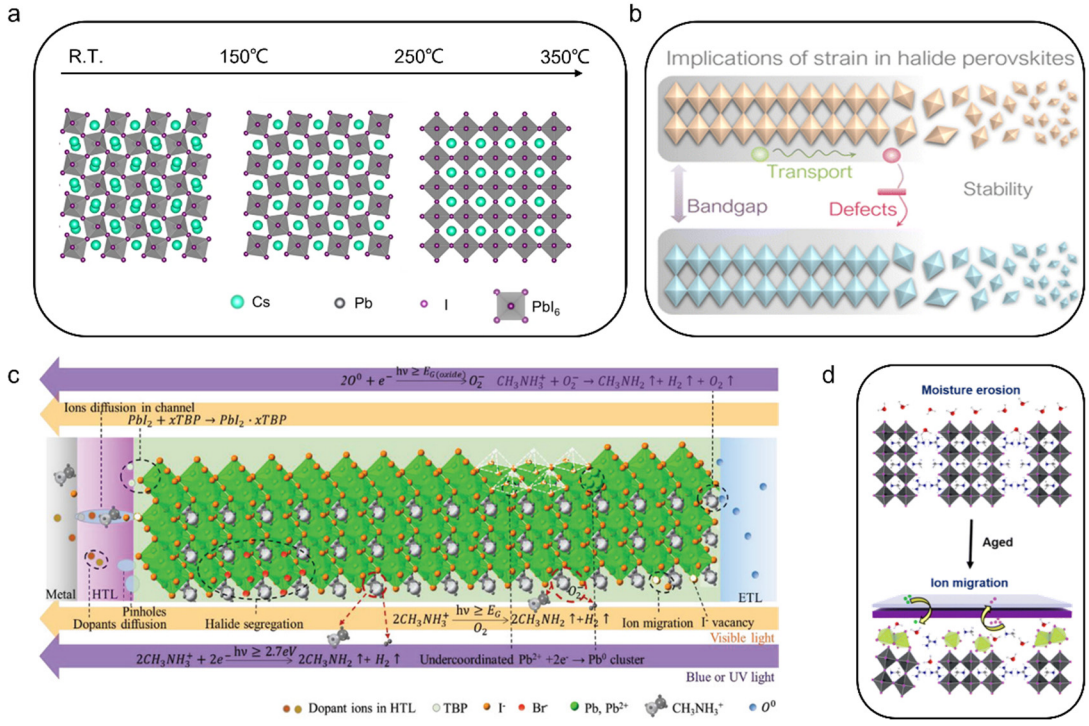

Figure 2. (**a**) Schematics of the thermal-induced change in the lattice of $CsPbI_3$ samples. Reprinted with permission from Ref. [23]. (**b**) Implications of strain on perovskite films. Reprinted with permission from Ref. [24]. (**c**) Impacts of visible, blue, and UV light illumination on PSCs. (E_G represents the bandgap of perovskite). Reprinted with permission from Ref. [25]. (**d**) Schematic diagram of perovskite films adsorbing water. Reprinted with permission from Ref. [26].

Under illumination, photoexcited carriers modify defect charge states and drive light-assisted ionic migration, while high-energy photons can directly induce bond cleavage and interfacial chemical reactions (Figure2c). These photoinduced effects are particularly pronounced at the perovskite/ETL interface, where electric fields, carrier accumulation, and chemical gradients are intrinsically coupled.

In parallel, environmental moisture interacts strongly with the ionic lattice, triggering hydration reactions, lattice swelling, and preferential degradation at interfacial regions with incomplete coordination or enhanced ion accessibility (Figure 2d). Such humidity-induced processes promote ion migration and chemical reconstruction at the interface, rather than uniform bulk degradation.

Collectively, temperature, strain, illumination and humidity do not act as isolated stressors but synergistically converge at the perovskite/ETL interface, rendering it the most dynamically active and vulnerable region in inverted perovskite solar cells. This intrinsic dynamic nature fundamentally challenges passivation strategies that rely on a fixed interfacial configuration, underscoring the need to reconsider interface design from a time-dependent and adaptive perspective.

3.1. Ion Migration and Photo-Induced Phase Separation

Among various forms of interfacial dynamic evolution, ion migration and photo-induced halide phase separation represent two closely coupled and mutually reinforcing destabilization mechanisms. Rather than acting as isolated bulk phenomena, these processes cooperatively drive the continuous reconstruction of interfacial structure, composition, and electrostatic landscape over operational time.

Under continuous illumination or electrical bias, the activation of halide ionic species, for example iodide in mixed-halide $MAPb(I_{1-x}Br_x)_3$, is generally enhanced, enabling directional ionic redistribution driven by internal electric fields and chemical potential gradients (Figure 3a). This ionic motion not only promote photo-induced halide phase separation but also perturbs local charge density and interfacial band bending, giving rise to iodide-rich and bromide-rich domains that evolve progressively under high excitation intensity [27]. Such coupled ionic and compositional rearrangements are now widely recognized as a fundamental source of interfacial instability rather than isolated bulk effects.

The consequences of this dynamic evolution are consistently reflected across electrical, optical, and structural characterizations. From an operational perspective, device parameters including PCE, J_{SC}, V_{OC}, and FF commonly exhibit pronounced scan-rate dependence after aging, with suppressed performance at slow scan rates and reduced hysteresis under fast sweeps (Figure 3b–e). This behavior is generally attributed to ion-induced field screening at functional interfaces, where accumulated mobile ions dynamically modulate the built-in electric field and charge-extraction barriers [28]. In parallel, time-dependent photoluminescence measurements frequently reveal red-shifted emission and intensity redistribution during prolonged illumination (Figure 3f), a characteristic optical signature of halide phase separation and the formation of low-bandgap iodide-rich domains that act as preferential recombination centers. Complementary PXRD analyses before and after illumination further corroborate this picture, with the emergence or evolution of diffraction features indicative of halide redistribution and lattice distortion (Figure 3g). Collectively, these recurring observations point to a continuous, time-dependent reconstruction of the perovskite interface, manifested through evolving interfacial dipoles, fluctuating electrostatic landscapes, and progressively enhanced interface-dominated recombination. Such intrinsically dynamic behavior fundamentally challenges the assumption of a static, permanently passivated interface, underscoring the limitations of conventional static passivation strategies under realistic operating conditions.

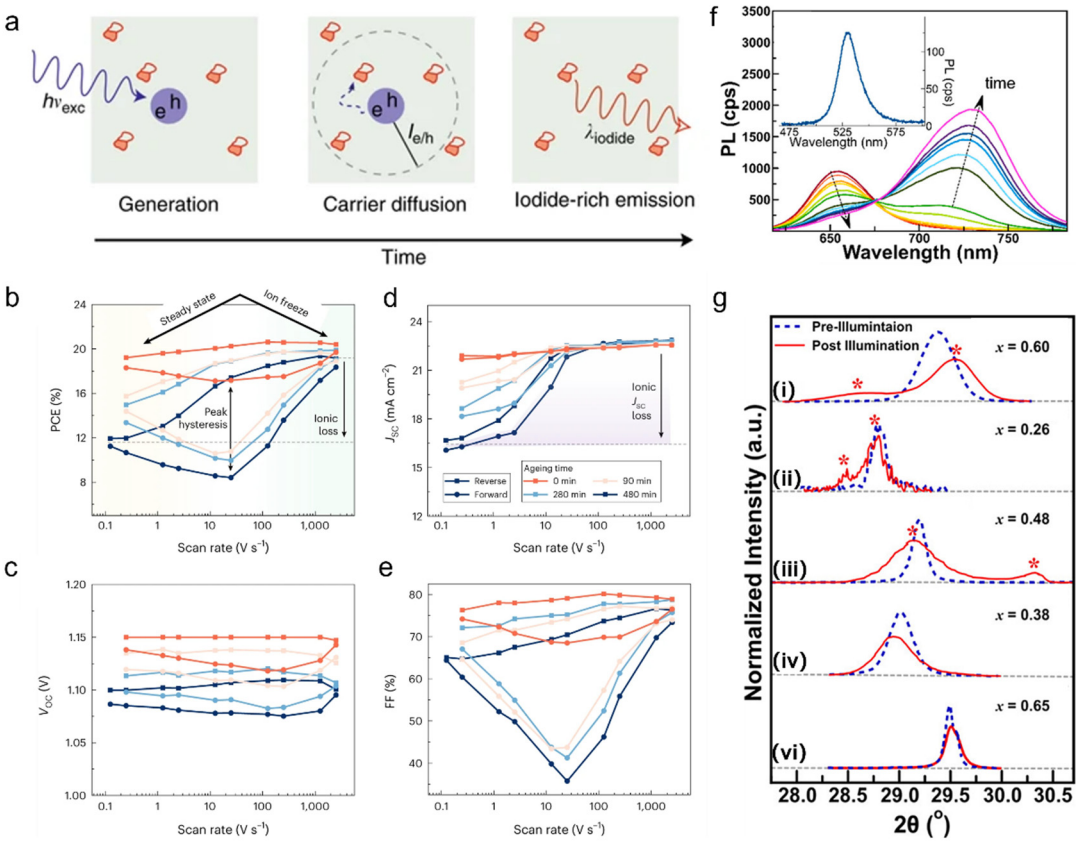

Figure 3. (**a**) High excitation intensity light-induced phase separation of $MAPb(I_{1-x}Br_x)_3$ (MA = $CH_3NH_3^+$). Reprinted with permission from Ref. [29]. The PCE (**b**), V_{OC} (**c**), J_{SC} (**d**) and FF (**e**) obtained from *J-V* characteristics measured at different scan speeds in reverse (squares) and forward (circles) scan direction for $Cs_{0.05}(FA_{0.83}MA_{0.17})_{0.95}Pb(I_{0.83}Br_{0.17})_3$ perovskite solar cells after different ageing times. Reprinted with permission from Ref. [30]. (**f**) Time evolution of $MAPb(I_{0.5}Br_{0.5})_3$ emission spectra under λ_{exc} = 405 nm CW excitation (I_{exc} = 20 mW cm^{-2}) over the course of 3 s. Times for selected spectra (from *red* to *purple*): 0.05, 1.41. 1.64, 1.69, 1.83, 1.93, 2.26, 2.40, 2.58, 2.68, 2.87, and 3.10 s. Inset: Emission spectrum between 475 and 600 nm indicative of Br-rich emission. Reprinted with permission from Ref. [29]. (**g**) Summary of $MAPb(I_{1-x}Br_x)_3$ literature pXRD powder patterns before (dashed blue) and after (solid red) illumination. Initial halide compositions given by x at the top right corner of each panel. Red asterisks denote post illumination peak positions for split I-rich and Br-rich domains. (i) reprinted with permission from Ref. [31]. (ii) reprinted with permission from Ref. [32]. (iii) reprinted with permission from Ref. [33]. (iv) reprinted with permission from Ref. [34]. (vi) reprinted with permission from Ref. [35].

3.2. Desorption of Passivating Molecules

Beyond ion migration and halide phase separation, the intrinsic instability of interface passivation layers constitutes another widely observed manifestation of dynamic interface evolution in perovskite solar cells. Under realistic operating conditions, passivation layers should not be regarded as chemically inert or permanently anchored components. Instead, they represent reactive and adaptive interfacial species whose molecular configuration, bonding state, and surface coverage can evolve continuously under illumination, thermal stress, and electrical bias [36]. In particular, increasing evidence shows that ultraviolet and high-energy visible photons can directly trigger chemical reactions or electronic excitation within commonly used organic passivators, initiating their gradual desorption or transformation (Figure 4a).

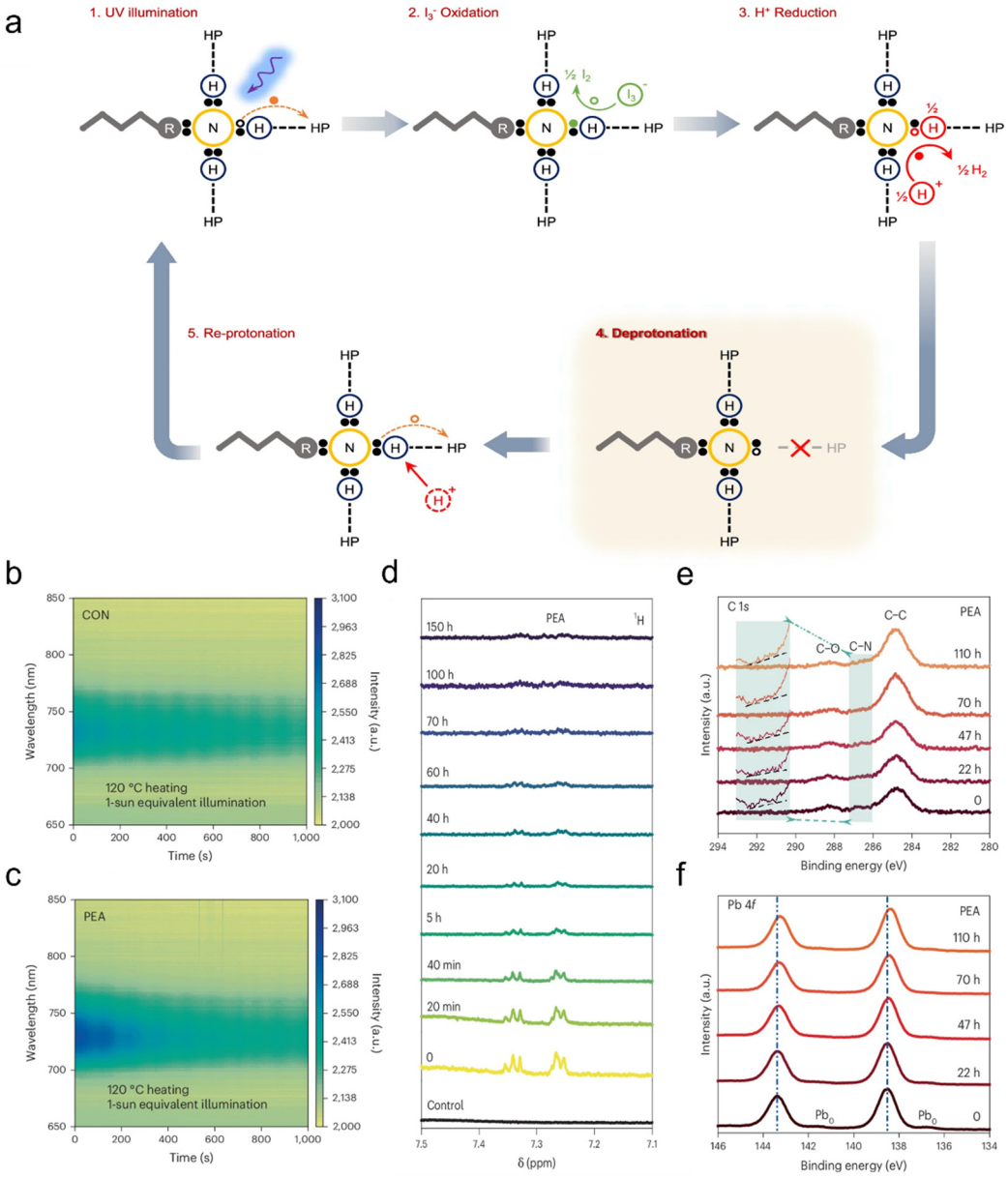

Figure 4. (**a**) Diagram of the violet/UV light-triggered photoreaction cycle. Hollow circles denote holes, solid circles denote electrons, and colored holes/electrons denote the charge carriers participating in the corresponding kinetics. Reprinted with permission from Ref. [36]. The evolution of the PL profile of as-prepared control (**b**), PEA^+ (**c**) perovskite films under continuous 120 °C heating and 1-sun equivalent illumination. (**d**) ^{1}H NMR spectra of control perovskite film, time-evolved ^{1}H NMR spectra of PEA^+ perovskite films under 100 °C heating and 1-sun equivalent illumination. δ denotes the chemical shift. (**e**,**f**) Evolution of the C 1s (**e**) and Pb 4f (**f**) XPS spectra of PEA^+ perovskite films under 100 °C heating and 1-sun equivalent illumination. The C-N signal is highlighted with green shading, and the green dashed lines are used to connect the two green shaded areas of the initial and enlarged regions. The black dashed lines in the left-hand side shade are guides to the eye, used to distinguish the changes in the C-N signal. The vertical dashed lines in (**f**) mark the initial binding energy position of the Pb 4f. Reprinted with permission from Ref. [37].

Representative experimental observations consistently reveal that passivators such as phenethylammonium (PEA^+), which are widely employed to suppress surface defects through ionic or coordinative interactions, undergo progressive desorption or chemical modification under operational conditions [37]. Time-dependent absorption spectroscopy under 1-sun illumination and elevated temperature shows pronounced spectral evolution for PEA-modified interfaces, in contrast to relatively stable control systems (Figure 4b,c), while the rapid decay and finally approaching the intensity close to the control film indicates the failure passivation effects of PEA^+ under continuous photothermal stress. Complementary solid-state characterizations further substantiate this dynamic behavior: 1H NMR spectra reveal a gradual attenuation of characteristic proton signals over extended aging

periods (Figure 4d). XPS analysis shows that the C–N peak of PEA^+ at 286.6 eV disappears after 22 h, indicating complete surface desorption of PEA^+, while deeper PEA^+ persists, and the Pb 4f shift confirms that PEA^+ does not inhibit perovskite surface chemical changes (Figure 4e,f). Collectively, these signatures point to a progressive loss or reconfiguration of passivation molecules at the interface rather than abrupt failure. Such desorption processes inevitably re-expose undercoordinated lead or halide sites, reactivate interfacial non-radiative recombination pathways, and facilitate subsequent ion accumulation, thereby accelerating device performance degradation. These observations underscore that interface passivation in perovskite solar cells is intrinsically dynamic, fundamentally challenging the conventional assumption of static and permanent defect passivation and highlighting the necessity of passivation strategies that explicitly account for chemical and structural evolution under operating conditions.

3.3. Interfacial Chemical Reactions and Electrode Corrosion

Once interface passivation integrity is progressively compromised, the perovskite/ETL interface can no longer be regarded as a chemically inert boundary but instead evolves into an increasingly reactive and structurally unstable region. Under the coupled influence of illumination, thermal stress, and electric-field-driven carrier injection, halide ions, especially iodide, tend to accumulate preferentially at grain boundaries and functional interfaces, where defect density and local electric fields are inherently higher. This enrichment leads to a pronounced increase in PbI_2 content at grain boundaries and interfaces, as directly visualized by high-resolution transmission electron microscopy, which reveals the gradual emergence and expansion of PbI_2-rich regions during aging (Figure 5a–c). Photoelectron spectroscopy further confirms this trend by showing a progressive deviation of the Pb/I atomic ratio from stoichiometry at degraded interfaces, indicating sustained halide depletion and chemical reconstruction rather than reversible ionic redistribution (Figure 5d). Together, these observations demonstrate that the interface undergoes a transition from defect-mediated electronic degradation to genuine chemical decomposition.

As halide depletion continues, mobile iodine species generated from perovskite decomposition, which include I^-, HI, and I_2, can further migrate across the ETL toward the top electrode under thermal stress and illumination. Upon reaching the Ag electrode, these iodine species readily participate in interfacial redox reactions with metallic Ag, leading to the formation of insulating AgI and establishing a chemically driven degradation pathway that couples ionic migration with electrode corrosion (Figure 5f). This process not only accelerates iodine loss from the perovskite lattice but also introduces a growing interfacial barrier for charge extraction, thereby amplifying both chemical and electrical instability.

As degradation proceeds, this chemically activated interface no longer evolves uniformly but instead propagates in a layer-by-layer manner [38]. At later stages, localized chemical reactions preferentially nucleate at pre-existing defects or weak points, progressively developing into pinholes and discontinuities that are clearly resolved in cross-sectional STEM images under accelerated thermal conditions (Figure 5g). These morphological failures permanently disrupt interfacial contact, resulting in abrupt losses in current density and V_{OC} and ultimately driving the device into an irreversible failure regime [39].

From an interfacial evolution perspective, these phenomena collectively represent the terminal manifestation of dynamic interface instability in perovskite solar cells. Chemical reactions, electrode corrosion, and morphological collapse do not occur as isolated degradation events but instead emerge from a self-amplifying interplay between ion migration, interfacial reactivity, and structural fragility. This final failure pathway underscores that perovskite interfaces are intrinsically dynamic systems whose chemical and morphological states continuously evolve under realistic operating conditions. Consequently, passivation strategies based solely on static defect coverage are fundamentally insufficient to prevent long-term degradation, highlighting the urgent need for interfacial designs that can suppress or accommodate chemically driven evolution throughout device operation.

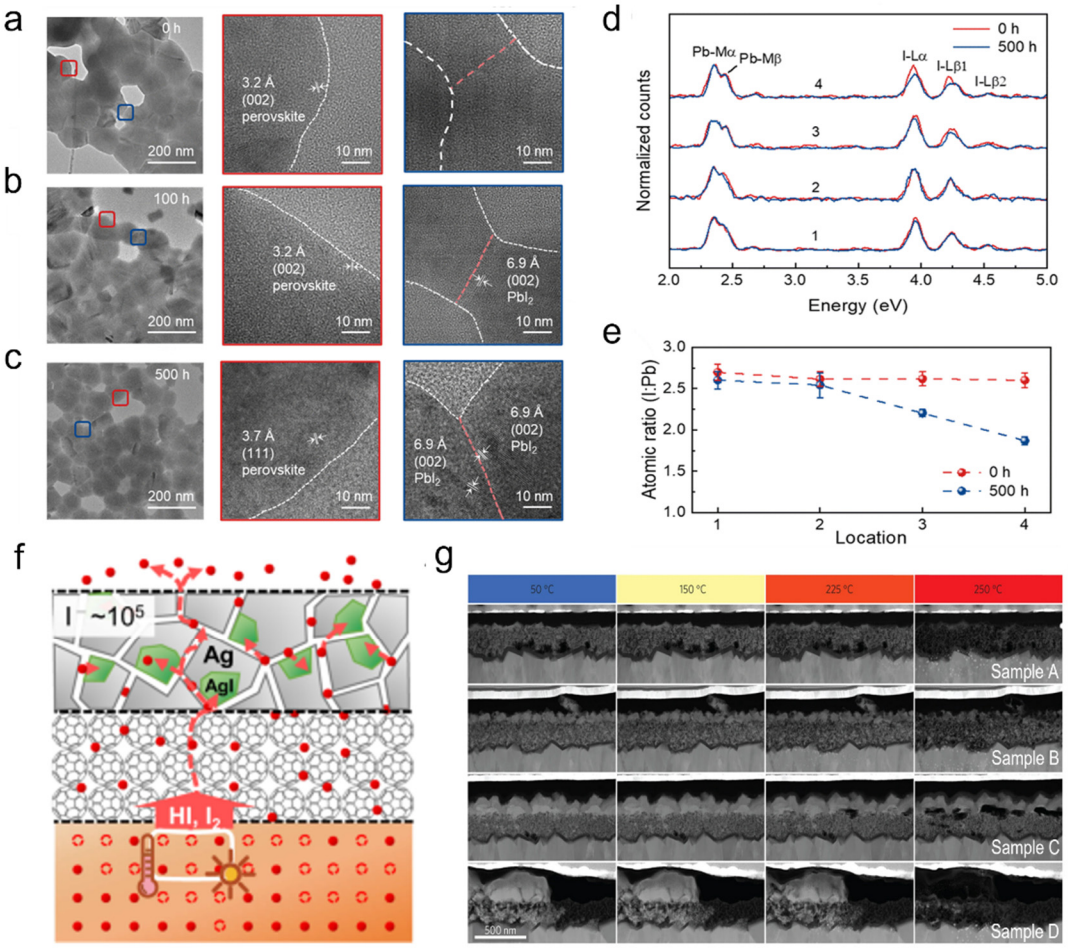

Figure 5. TEM images and the corresponding enlarged views of the perovskite films under AM 1.5G illumination for (**a**) 0 h, (**b**) 100 h, and (**c**) 500 h. The regions highlighted in red and blue boxes indicate the non-contacted and contacted GBs, respectively. (**d**) EDS profiles of the four different regions before and after light illumination. Bulk grains, non-contacted GBs, contacted GBs without PbI_2, and contacted GBs with PbI_2 are represented by 1, 2, 3, and 4, respectively. (**e**) Atomic I: Pb ratios in the four regions determined by EDS before and after light illumination. Reprinted with permission from Ref. [40]. (**f**) Schematic diagram of the iodine ions migration within the devices with Ag. Reprinted with permission from Ref. [41]. (**g**) A high-angle annular dark-field (HAADF) imaging technique to study the sample at various heating stages. Reprinted with permission from Ref. [42].

4. Dynamic Interface-Oriented Strategies and Outlook

The above analysis indicates that the interface between the perovskite absorber and the ETL undergoes a series of dynamically coupled transformations during real device operation. These include sustained ion migration, interfacial structural reconstruction, passivator destabilization, chemically driven interfacial reactions, and localized micro-fracturing or partial delamination. Rather than occurring independently, these processes interact and reinforce one another, collectively governing the long-term operational stability of perovskite solar cells. However, prevailing interface passivation strategies remain predominantly rooted in the assumption that the interface is static and thus chemically and structurally invariant once initially optimized. Such a framework struggles to account for the continuous evolution of interfacial states under prolonged exposure to light, heat, and electrical bias. Consequently, future interface engineering must shift its core objective from maximizing initial passivation efficacy toward developing interface systems capable of sustaining functional stability under dynamic photothermal and electrical operating conditions.

At the stage of materials screening, theoretical modelling and data-driven approaches should go beyond predicting static interfacial configurations and instead prioritize the evolution pathways and stability windows of interfaces under realistic operating stresses [43]. By integrating high-throughput computation with machine learning models, it is possible to simultaneously assess the intrinsic stability of interface materials, their chemical compatibility with perovskite and transport layers, and their ability to maintain dynamically stable interfaces under temperature,

humidity, and bias perturbations [44]. This shift from evaluating single-point performance to predicting evolutionary behavior will establish a theoretical foundation for addressing long-term dynamic interface failure.

Beyond predictive screening, interface material design itself must embrace controlled dynamics. Recent studies on thermally or environmentally activated dynamic passivation systems provide compelling experimental evidence for the feasibility to develop an adaptive interface. In such a system, reversible chemical bonds or latent Lewis-base precursor motifs can be activated under illumination, heating, or hydrothermal stress, enabling the formation of new coordination or bonding sites in response to freshly generated interfacial defects [45]. This dynamic defect compensation mechanism allows for sustained passivation during ongoing interfacial evolution, effectively delaying performance degradation under harsh operating conditions. These findings demonstrate that the interface does not need to be chemically static; instead, deliberately engineered reconfigurability can preserve low defect densities and stable charge transport over extended operation.

In parallel, the construction of gradient and multilayer interfacial architectures offers an effective strategy to mitigate interfacial chemical reactions and morphological degradation. Compared with single-layer passivation schemes, gradient or multilayer interface can spatially decouple ion accumulation zones, charge transport regions, and reaction-sensitive areas, thereby reducing local chemical potential build-up and suppressing reaction driving forces. Rationally designed gradients in energy level alignment, composition, or polarity can also modulate the migration pathways and local accumulation tendencies of halide ions and charge carriers, diminishing the formation of reactive phases and lowering the risk of electrode corrosion. Moreover, by dispersing localized stresses associated with ion migration and lattice mismatch, such architectures can suppress pinhole expansion and interfacial fracture, enhancing both structural and electrical robustness during long-term operation.

Ultimately, a comprehensive understanding and effective regulation of dynamic interfaces rely on in situ and real-time characterization techniques tailored to realistic working conditions. Conventional pre- and post-ageing comparisons often obscure the initial triggers and critical transition stages of interfacial evolution. In contrast, concurrent in situ spectroscopic, microscopic, and compositional analyses performed under illumination, electrical bias, and thermal stress enable direct observation of ion migration, reactive phase formation, and defect state evolution [46]. These time-resolved insights are essential not only for elucidating failure mechanisms but also for establishing quantitative correlations between interfacial dynamics and performance degradation, thereby feeding back into predictive and data-driven design frameworks (Figure 6).

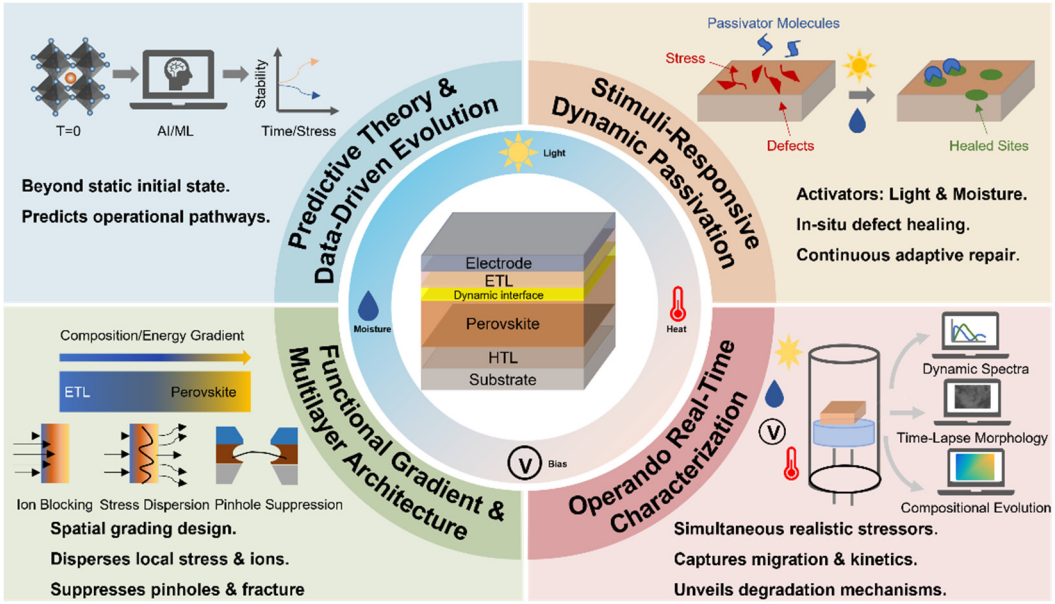

Figure 6. Strategies for dynamic perovskite/ETL interface.

In summary, interface engineering between the perovskite layer and the electron transport layer is undergoing a necessary paradigm shift. Interfaces should no longer be regarded as static structures requiring permanent chemical stability, but rather as dynamically evolving systems whose functionality can be actively regulated during operation. Through the coordinated advancement of predictive modelling, adaptive material design, and in situ characterization, it is increasingly feasible to develop genuinely dynamic passivation and regulation strategies. Such approaches hold the key to overcoming the fundamental stability constraints imposed by interfaces and to enabling the long-term operational reliability of perovskite solar cells.

Author Contributions: J.X. and R.W. directed and supervised the project. Q.X. conceived the idea and wrote the manuscript. X.J., X.W. and Q.L. assisted with the content modification. All authors have read and agreed to the published version of the manuscript.

Funding: This work was supported by the National Natural Science Foundation of China (grant no. 62474143), the Scientific Research Innovation Capability Support Project for Young Faculty (SRICSPYF-BS2025014), Natural Science Foundation of Zhejiang Province of China (grant nos. LD24E020001 and QKWL25E1301), and support from the Key R&D Program of Zhejiang (2024SSYS0061). J.X. acknowledges grants (grant nos. LR24F040001, LDG25E020001) from the Natural Science Foundation of Zhejiang Province of China, the grant from the National Natural Science Foundation of China (grant no. 62274146), the support from the Fundamental Research Funds for the Central Universities (226-2022-00200), the grant from the Research and Development Foundation of Dongfang Electric (Hangzhou) Innovation Institute Co., Ltd. (grant no. 4F-CSC24005), and Zhejiang Province's Vanguard and Leader Geese Research and Development Program (2024C01246(SD2)).

Data Availability Statement: Not applicable.

Conflicts of Interest: The authors declare no conflict of interest.

Use of AI and AI-Assisted Technologies: During the preparation of this work, the authors used ChatGPT to polish the language of the article. After using this tool, the authors reviewed and edited the content as needed and take full responsibility for the content of the published article.

References

1. Rajagopal, A.; Yao, K.; Jen, A.K.Y. Toward Perovskite Solar Cell Commercialization: A Perspective and Research Roadmap Based on Interfacial Engineering. *Adv. Mater.* **2018**, *30*, 1800455. https://doi.org/10.1002/adma.201800455.
2. Kim, D.H.; Park, N.-G. Advanced Interface Engineering for Perovskite Solar Cells: The Way to Ensure Efficiency and Stability. *Acc. Mater. Res.* **2025**, *6*, 1147–1157. https://doi.org/10.1021/accountsmr.5c00170.
3. Tao, J.; Zhao, C.; Wang, Z.; Chen, Y.; Zang, L.; Yang, G.; Bai, Y.; Chu, J. Suppressing non-radiative recombination for efficient and stable perovskite solar cells. *Energy Environ. Sci.* **2025**, *18*, 509–544. https://doi.org/10.1039/D4EE02917H.
4. Shin, S.S.; Park, B.; Noh, J.H.; Seok, S.I. Interlayer engineering in metal halide perovskite photovoltaics. *Nat. Photonics* **2026**, *20*, 11–23. https://doi.org/10.1038/s41566-025-01809-8.
5. Shen, Y.; Zhang, T.; Xu, G.; Steele, J.A.; Chen, X.; Chen, W.; Zheng, G.; Li, J.; Guo, B.; Yang, H.; et al. Strain regulation retards natural operation decay of perovskite solar cells. *Nature* **2024**, *635*, 882–889. https://doi.org/10.1038/s41586-024-08161-x.
6. Jin, B.; Cao, J.; Yuan, R.; Cai, B.; Wu, C.; Zheng, X. Strain Relaxation for Perovskite Lattice Reconfiguration. *Adv. Energy Sustain. Res.* **2023**, *4*, 2200143. https://doi.org/10.1002/aesr.202200143.
7. Lin, Z.; Zhang, W.; Cai, Q.; Xu, X.; Dong, H.; Mu, C.; Zhang, J.-P. Precursor Engineering of the Electron Transport Layer for Application in High-Performance Perovskite Solar Cells. *Adv. Sci.* **2021**, *8*, 2102845. https://doi.org/10.1002/advs.202102845.
8. Luo, D.; Su, R.; Zhang, W.; Gong, Q.; Zhu, R. Minimizing non-radiative recombination losses in perovskite solar cells. *Nat. Rev. Mater.* **2020**, *5*, 44–60. https://doi.org/10.1038/s41578-019-0151-y.
9. Kang, J.; Li, J.; Wei, S.-H. Atomic-scale understanding on the physics and control of intrinsic point defects in lead halide perovskites. *Appl. Phys. Rev.* **2021**, *8*, 031302. https://doi.org/10.1063/5.0052402.
10. Chen, H.; Zhang, W.; Li, M.; He, G.; Guo, X. Interface Engineering in Organic Field-Effect Transistors: Principles, Applications, and Perspectives. *Chem. Rev.* **2020**, *120*, 2879–2949. https://doi.org/10.1021/acs.chemrev.9b00532.
11. Li, J.; Jin, C.; Jiang, R.; Su, J.; Tian, T.; Yin, C.; Meng, J.; Kou, Z.; Bai, S.; Müller-Buschbaum, P.; et al. Homogeneous coverage of the low-dimensional perovskite passivation layer for formamidinium–caesium perovskite solar modules. *Nat. Energy* **2024**, *9*, 1540–1550. https://doi.org/10.1038/s41560-024-01667-8.
12. Guan, H.; Zhang, W.; Liang, J.; Wang, C.; Hu, X.; Pu, D.; Huang, L.; Ge, Y.; Cui, H.; Zou, Y.; et al. Low-Dimensional 2-thiopheneethylammonium Lead Halide Capping Layer Enables Efficient Single-Junction Methylamine-Free Wide-Bandgap and Tandem Perovskite Solar Cells. *Adv. Funct. Mater.* **2023**, *33*, 2300860. https://doi.org/10.1002/adfm.202300860.
13. Su, R.; Xu, Z.; Wu, J.; Luo, D.; Hu, Q.; Yang, W.; Yang, X.; Zhang, R.; Yu, H.; Russell, T.P.; et al. Dielectric screening in perovskite photovoltaics. *Nat. Commun.* **2021**, *12*, 2479. https://doi.org/10.1038/s41467-021-22783-z.
14. Chen, B.; Rudd, P.N.; Yang, S.; Yuan, Y.; Huang, J. Imperfections and their passivation in halide perovskite solar cells. *Chem. Soc. Rev.* **2019**, *48*, 3842–3867. https://doi.org/10.1039/C8CS00853A.
15. Liu, C.; Yang, Y.; Chen, H.; Xu, J.; Liu, A.; Bati, A.S.R.; Zhu, H.; Grater, L.; Hadke, S.S.; Huang, C.; et al. Bimolecularly passivated interface enables efficient and stable inverted perovskite solar cells. *Science* **2023**, *382*, 810–815. https://doi.org/10.1126/science.adk1633.
16. Wu, G.; Liang, R.; Ge, M.; Sun, G.; Zhang, Y.; Xing, G. Surface Passivation Using 2D Perovskites toward Efficient and Stable Perovskite Solar Cells. *Adv. Mater.* **2022**, *34*, 2105635. https://doi.org/10.1002/adma.202105635.
17. Tress, W.; Domanski, K.; Carlsen, B.; Agarwalla, A.; Alharbi, E.A.; Graetzel, M.; Hagfeldt, A. Performance of perovskite solar cells under simulated temperature-illumination real-world operating conditions. *Nat. Energy* **2019**, *4*, 568–574.

https://doi.org/10.1038/s41560-019-0400-8.

18. Wu, L.; Hu, S.; Yang, F.; Li, G.; Wang, J.; Zuo, W.; Jerónimo-Rendon, J.J.; Turren-Cruz, S.-H.; Saba, M.; Saliba, M.; et al. Resilience pathways for halide perovskite photovoltaics under temperature cycling. *Nat. Rev. Mater.* **2025**, *10*, 536–549. https://doi.org/10.1038/s41578-025-00781-7.
19. Zhu, H.; Teale, S.; Lintangpradipto, M.N.; Mahesh, S.; Chen, B.; McGehee, M.D.; Sargent, E.H.; Bakr, O.M. Long-term operating stability in perovskite photovoltaics. *Nat. Rev. Mater.* **2023**, *8*, 569–586. https://doi.org/10.1038/s41578-023-00582-w.
20. Hu, J.; Chen, P.; Luo, D.; Wang, D.; Chen, N.; Yang, S.; Fu, Z.; Yu, M.; Li, L.; Zhu, R.; et al. Tracking the evolution of materials and interfaces in perovskite solar cells under an electric field. *Commun. Mater.* **2022**, *3*, 39. https://doi.org/10.1038/s43246-022-00262-2.
21. Meggiolaro, D.; Motti, S.G.; Mosconi, E.; Barker, A.J.; Ball, J.; Andrea Riccardo Perini, C.; Deschler, F.; Petrozza, A.; De Angelis, F. Iodine chemistry determines the defect tolerance of lead-halide perovskites. *Energy Environ. Sci.* **2018**, *11*, 702–713. https://doi.org/10.1039/C8EE00124C.
22. Li, Z.; Jia, C.; Wu, H.; Tang, Y.; Zhao, J.; Su, Z.; Gao, X.; Qiu, S.; Yuan, H.; Li, M. In-Situ Cross-Linked Polymers for Enhanced Thermal Cycling Stability in Flexible Perovskite Solar Cells. *Angew. Chem. Int. Ed.* **2025**, *64*, e202421063. https://doi.org/10.1002/anie.202421063.
23. Ma, M.; Zhang, X.; Chen, X.; Xiong, H.; Xu, L.; Cheng, T.; Yuan, J.; Wei, F.; Shen, B. In situ imaging of the atomic phase transition dynamics in metal halide perovskites. *Nat. Commun.* **2023**, *14*, 7142. https://doi.org/10.1038/s41467-023-42999-5.
24. Yang, B.; Bogachuk, D.; Suo, J.; Wagner, L.; Kim, H.; Lim, J.; Hinsch, A.; Boschloo, G.; Nazeeruddin, M.K.; Hagfeldt, A. Strain effects on halide perovskite solar cells. *Chem. Soc. Rev.* **2022**, *51*, 7509–7530. https://doi.org/10.1039/D2CS00278G.
25. Wei, J.; Wang, Q.; Huo, J.; Gao, F.; Gan, Z.; Zhao, Q.; Li, H. Mechanisms and Suppression of Photoinduced Degradation in Perovskite Solar Cells. *Adv. Energy Mater.* **2021**, *11*, 2002326. https://doi.org/10.1002/aenm.202002326.
26. Xing, Z.; Fan, B.; Meng, X.; Li, D.; Huang, Z.; Li, L.; Zhang, Y.; Wang, F.; Hu, X.; Hu, T.; et al. Repairing humidity-induced interfacial degradation in quasi-2D perovskite solar cells printed in ambient air. *Energy Environ. Sci.* **2024**, *17*, 3660–3669. https://doi.org/10.1039/D4EE00912F.
27. Lan, Z.; Yang, Y.; Huang, H.; Du, S.; Zhang, Q.; Wang, Z.; Jiang, T.; Sun, C.; Qu, S.; Li, L.; et al. Interfacial electrostatic repulsion inhibits iodide ion migration for enhancing reverse-bias stability of perovskite solar cells. *Nat. Commun.* **2025**, *16*, 11407. https://doi.org/10.1038/s41467-025-66224-7.
28. Xu, J.; Boyd, C.C.; Yu, Z.J.; Palmstrom, A.F.; Witter, D.J.; Larson, B.W.; France, R.M.; Werner, J.; Harvey, S.P.; Wolf, E.J.; et al. Triple-halide wide–band gap perovskites with suppressed phase segregation for efficient tandems. *Science* **2020**, *367*, 1097–1104. https://doi.org/10.1126/science.aaz5074.
29. Draguta, S.; Sharia, O.; Yoon, S.J.; Brennan, M.C.; Morozov, Y.V.; Manser, J.S.; Kamat, P.V.; Schneider, W.F.; Kuno, M. Rationalizing the light-induced phase separation of mixed halide organic–inorganic perovskites. *Nat. Commun.* **2017**, *8*, 200. https://doi.org/10.1038/s41467-017-00284-2.
30. Thiesbrummel, J.; Shah, S.; Gutierrez-Partida, E.; Zu, F.; Peña-Camargo, F.; Zeiske, S.; Diekmann, J.; Ye, F.; Peters, K.P.; Brinkmann, K.O.; et al. Ion-induced field screening as a dominant factor in perovskite solar cell operational stability. *Nat. Energy* **2024**, *9*, 664–676. https://doi.org/10.1038/s41560-024-01487-w.
31. Hoke, E.T.; Slotcavage, D.J.; Dohner, E.R.; Bowring, A.R.; Karunadasa, H.I.; McGehee, M.D. Reversible photo-induced trap formation in mixed-halide hybrid perovskites for photovoltaics. *Chem. Sci.* **2015**, *6*, 613–617. https://doi.org/10.1039/C4SC03141E.
32. Hu, M.; Bi, C.; Yuan, Y.; Bai, Y.; Huang, J. Stabilized Wide Bandgap $MAPbBr_xI_{3-x}$ Perovskite by Enhanced Grain Size and Improved Crystallinity. *Adv. Sci.* **2016**, *3*, 1500301. https://doi.org/10.1002/advs.201500301.
33. Duong, T.; Mulmudi, H.K.; Wu, Y.; Fu, X.; Shen, H.; Peng, J.; Wu, N.; Nguyen, H.T.; Macdonald, D.; Lockrey, M.; et al. Light and Electrically Induced Phase Segregation and Its Impact on the Stability of Quadruple Cation High Bandgap Perovskite Solar Cells. *ACS Appl. Mater. Interfaces* **2017**, *9*, 26859–26866. https://doi.org/10.1021/acsami.7b06816.
34. Yang, Z.; Rajagopal, A.; Jo, S.B.; Chueh, C.C.; Williams, S.; Huang, C.C.; Katahara, J.K.; Hillhouse, H.W.; Jen, A.K.Y. Stabilized Wide Bandgap Perovskite Solar Cells by Tin Substitution. *Nano Lett.* **2016**, *16*, 7739–7747. https://doi.org/10.1021/acs.nanolett.6b03857.
35. Barker, A.J.; Sadhanala, A.; Deschler, F.; Gandini, M.; Senanayak, S.P.; Pearce, P.M.; Mosconi, E.; Pearson, A.J.; Wu, Y.; Srimath Kandada, A.R.; et al. Defect-Assisted Photoinduced Halide Segregation in Mixed-Halide Perovskite Thin Films. *ACS Energy Lett.* **2017**, *2*,1416–1424. https://doi.org/10.1021/acsenergylett.7b00282.
36. Yu, D.; Cao, F.; Qiu, X.; Chen, Y.; Zhang, Z.; Wang, G.; Mao, Y.; Zhong, J.; Su, C.; Huang, W.; et al. Violet/ultraviolet light-induced depassivation in halide perovskite solar cells. *Nat. Commun.* **2025**, *16*, 11409. https://doi.org/10.1038/s41467-025-66227-4.
37. Pei, F.; Lin, S.; Zhang, Z.; Lin, S.; Huang, X.; Zhao, M.; Xu, J.; Zhuang, X.; Zhang, Y.; Tang, J.; et al. Inhibiting defect passivation failure in perovskite for perovskite/Cu(In,Ga)Se2 monolithic tandem solar cells with certified efficiency

27.35%. *Nat. Energy* **2025**, *10*, 824–835. https://doi.org/10.1038/s41560-025-01761-5.

38. Li, H.; Xie, G.; Fang, J.; Peng, H.; Huang, N.; Wang, X.; Lin, D.; Qiu, L. Revealing the Relationship between Interfacial Morphology Degradation and Unsatisfied Stability in Phenethylamine-Treated Perovskite Solar Cell. *Small* **2025**, *21*, e03623. https://doi.org/10.1002/smll.202503623.
39. Li, X.; Fu, S.; Zhang, W.; Ke, S.; Song, W.; Fang, J. Chemical anti-corrosion strategy for stable inverted perovskite solar cells. *Sci. Adv.* **2020**, *6*, eabd1580. https://doi.org/10.1126/sciadv.abd1580.
40. Wang, H.; Li, Q.; Zhu, Y.; Sui, X.; Fan, X.; Lin, M.; Shi, Y.; Zheng, Y.; Yuan, H.; Zhou, Y.; et al. Photomechanically accelerated degradation of perovskite solar cells. *Energy Environ. Sci.* **2025**, *18*, 2254–2263. https://doi.org/10.1039/D4EE04878D.
41. Zhou, J.; Liu, Z.; Yu, P.; Tong, G.; Chen, R.; Ono, L.K.; Chen, R.; Wang, H.; Ren, F.; Liu, S.; et al. Modulation of perovskite degradation with multiple-barrier for light-heat stable perovskite solar cells. *Nat. Commun.* **2023**, *14*, 6120. https://doi.org/10.1038/s41467-023-41856-9.
42. Divitini, G.; Cacovich, S.; Matteocci, F.; Cinà, L.; Di Carlo, A.; Ducati, C. In situ observation of heat-induced degradation of perovskite solar cells. *Nat. Energy* **2016**, *1*, 15012. https://doi.org/10.1038/nenergy.2015.12.
43. Correa-Baena, J.-P.; Hippalgaonkar, K.; van Duren, J.; Jaffer, S.; Chandrasekhar, V.R.; Stevanovic, V.; Wadia, C.; Guha, S.; Buonassisi, T. Accelerating Materials Development via Automation, Machine Learning, and High-Performance Computing. *Joule* **2018**, *2*, 1410–1420. https://doi.org/10.1016/j.joule.2018.05.009.
44. Zhang, C.; Jia, Y.; Zhang, B.; Zhao, Q.; Xu, R.; Pang, S.; Wang, H.; De Wolf, S.; Wang, K. Machine learning-driven interface material design for high-performance perovskite solar cells with scalability and band-gap universality. *Joule* **2025**, *10*, 102264. https://doi.org/10.1016/j.joule.2025.102264.
45. Wang, W.-T.; Holzhey, P.; Zhou, N.; Zhang, Q.; Zhou, S.; Duijnstee, E.A.; Rietwyk, K.J.; Lin, J.-Y.; Mu, Y.; Zhang, Y.; et al. Water- and heat-activated dynamic passivation for perovskite photovoltaics. *Nature* **2024**, *632*, 294–300. https://doi.org/10.1038/s41586-024-07705-5.
46. Mao, L.; Xiang, C. A comprehensive review of machine learning applications in perovskite solar cells: Materials discovery, device performance, process optimization and systems integration. *Mater. Today Energy* **2025**, *47*, 101742. https://doi.org/10.1016/j.mtener.2024.101742.